LANGMUIR Article
Cite This: Langmuir 2018, 34, 10684−10693
pubs.acs.org/Langmuir

Biodegradable Poly(L-lactic acid) (PLLA) Coatings Fabricated from Nonsolvent Induced Phase Separation for Improving Corrosion Resistance of Magnesium Rods in Biological Fluids

Yifeng Sheng,[†] Li Tian,[‡] Chi Wu,[†] Ling Qin,*[,‡] and To Ngai*[,†]

[†]Department of Chemistry, The Chinese University of Hong Kong, Shatin, N. T. Hong Kong, China
[‡]Musculoskeletal Research Laboratory, Department of Orthopaedics and Traumatology, and Innovative Orthopaedic Biomaterial and Drug Translational Research Laboratory of Li Ka Shing Institute of Health, Faculty of Medicine, The Chinese University of Hong Kong, Shatin, N. T. Hong Kong, China

ABSTRACT: Magnesium (Mg)-based biometals are increasingly becoming a promising candidate of the next-generation implantable materials due to their unique properties, such as high biocompatibility, favorable mechanical strength, and good biodegradability in physiological conditions. However, the swift corrosion of Mg, resulting in early loss of structural support, has posed an enormous challenge in clinical application of Mg-based implants. To overcome these limitations, herein we developed a novel method, which combines the traditional dip-coating with nonsolvent induced phase separation (NIPS), to fabricate biodegradable PLLA coatings with controlled membrane morphology on pure Mg rods. Unlike the conventional dip-coating, where the polymer solution on the Mg substrates is left to evaporate directly under proper atmosphere, in NIPS, the polymer solution on the substrates is not left to dry but immersed in a nonsolvent of the PLLA, leading to the precipitation of polymer networks. Our results demonstrated that various polymer coatings with different morphologies and inner structures could be easily fabricated by a careful selection of nonsolvents. In comparison to dense PLLA coatings obtained from conventional solvent evaporation, PLLA coatings with a dense surface and porous inner structure were obtained when hexane and petroleum ether were used as the nonsolvents, while PLLA coatings with a completely porous structure were obtained when polar acetone and ethanol were chosen. The electrochemical corrosion tests and immersion tests further showed that all polymer coatings could significantly improve the corrosion resistance and suppress the corrosion rates of the substrates. However, PLLA films obtained via NIPS had much lower pH changes and slower Mg^{2+} release, implying better protective effects of the fabricated coatings. Based on results of all experiments, a new process for the corrosion mechanism of Mg implants during immersion has also been proposed in this work.

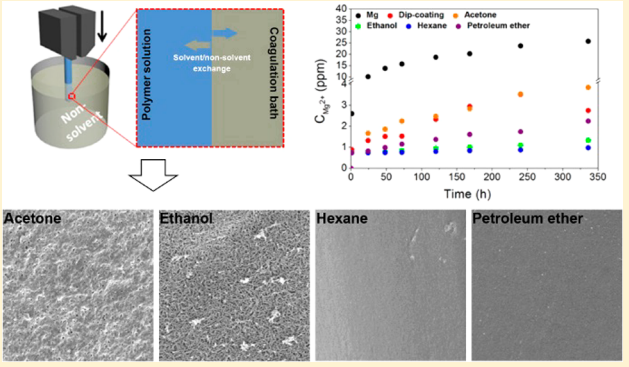

INTRODUCTION

Orthopedic problems, such as bone fractures, osteoporosis, and osteoarthritis are becoming major challenges in our health care system, which greatly stimulates the development of implants, of which alloy-based implants are the most commonly used.[1−3] However, their poor biocompatibility, unfavorable mechanical strength, and nonbiodegradation still remain major problems to become ideal implants.[4−6] For example, due to the mismatched elastic moduli, most of the metal based implants would result in stress shielding effects.[7] More importantly, an extra surgery will be often required to remove the implants in order to avoid potential adverse effects after fracture healing, which further causes pain to the patients.[4] To seek for novel biomaterials for improved implant devices, biodegradable polymers, e.g., poly(L-lactic acid) (PLLA), poly(glycolide) (PGA), and their copolymer poly(lactic-*co*-glycolic acid) (PLGA), have gained attention. However, due to their insufficient mechanical strength or brittleness, surgery failure may occur when using these polymers as the implant devices. In addition, it has been reported that the complete degradation of these polymer devices is unfavorable for osteogenesis and osseous ingrowth.[8]

In recent years, magnesium (Mg) and its alloys are becoming an appealing choice as new implantable materials in the orthopedic surgery to mitigate the current drawbacks of metallic and polymeric implants. Taking advantage of their tensile strength, along with compressive yield strength and Young's modulus, which are similar to that of natural bone, they could greatly alleviate or even eliminate the stress shielding effects.[9] More importantly, they are biodegradable so that patients could avoid a secondary surgery for implant removal upon the completion of the fracture healing. In

Received: July 10, 2018
Revised: August 17, 2018
Published: August 20, 2018

DOI: 10.1021/acs.langmuir.8b02322
Langmuir 2018, 34, 10684−10693

addition, the release of Mg ions during implantation is known to promote the growth of new bones.[10] However, their low corrosion resistance, associated with fast hydrogen release and rapid pH increase, which could largely undermine the implant lifetime, has posed the foremost obstacle on its way toward clinical applications.[9,11−14] Furthermore, the excessive degradation of Mg would cause severe risk of secondary fracture, since implants would lose their mechanical integrity before the tissue completely heals.[15]

To overcome these limitations, various strategies, including alloying, surface modification and coatings, etc., have been applied to enhance the corrosion resistance of pure Mg and its alloys.[16−21] Of these methods, polymer coatings, which can simultaneously control Mg degradation and improve its biocompatibility, are consequently receiving increasing attention, due to their ease of preparation, high efficiency, and a wide range of polymer choices. In 2010, Wong et al. first reported the fabrication of porous poly(caprolactone) (PCL) coatings on AZ91 Mg alloys via the spray-coating method.[22] With controlled flow and temperature, PCL coatings with different porosity could be fabricated and they demonstrated that PCL coatings could enhance both the corrosion resistance and biocompatibility of the Mg substrates, while coated Mg implants would more effectively promote bone growth after surgery. However, whether nonporous PCL coatings would have an even better corrosion resistance had not been demonstrated in this study. In another study reported by Li et al.,[23] PLGA with different thicknesses were deposited onto Mg−6Zn alloys via dip-coating by changing the concentration of polymer solutions. PLGA coatings, which provided protection to the substrates, also helped cells to attach, spread, and immigrate on the substrates. However, thinner PLGA coatings were found to perform better than thicker coatings, which may be due to the poor quality of thick coatings, indicating that the whole degradation was a comprehensive result of breakdown of the protective layer and self-passivation of the substrate. Xu et al. have further studied both PLA and PCL coatings with nonporous structure on pure Mg via spin-coating.[24] In their work, they found that the coating thickness mainly depended on the molecular weight of the polymers under identical spin speed and they showed that PLA coatings had stronger adhesion to the substrate in comparison to PCL coatings. In contrast, thicker polymer coatings showed significantly improved biocompatibility compared to thinner coatings in the cell culture test. However, the influence on the formation of corrosion products was not reported in this study. In addition, Abdal-hay demonstrated a comparison between porous PLA coating via dip-coating and three-dimensional PLA architecture by electrospinning.[25] Their results illustrated that three-dimensional PLA architectures were more suitable for long-term protection, since they were attributed to the deposition of Ca/Mg/P minerals, removal of the formed hydrogen, and maintenance of coating integration. Besides, the large surface area of the three-dimensional architectures equipped the Mg alloys with more excellent bioactivity for cell adhesion and proliferation at a long culture time. However, these three-dimensional PLA coated samples had comparatively faster initial corrosion rates due to their higher porosity. Another remarkable issue was their assumption that PLA films induced by dip-coating, which were composed of a dense inner bulk and a porous surface, would greatly suffer from bursting or delamination of the coatings, as the dense polymer network lacked sufficient permeability to transfer the excessive corrosion products. A similar phenomenon was also reported by Scharnagl,[26] which demonstrated AZ31 with microporous PEI coating had better corrosion resistance, since the accumulative hydrogen bubbles and salts caused cracking and detachment of polymer coatings. Although previous investigations demonstrated that polymer coatings could improve the initial corrosion resistance of magnesium, only limited success has been achieved in producing long-lasting Mg-based implants, since most of the reported coatings were either too porous or too dense. For porous coatings, body fluid could easily pass through the porous films, causing fast corrosion immediately after immersion.[27,28] However, densely packed inner structures would result in poor dredging of hydrogen gas and fast burst of membranes.[25,29] Thus, formation of favorable polymer coatings with controlled morphology and structure is essential for maintaining long-term degradation resistance of Mg-based implants.

To better control polymer coating formation, an alternative method based on nonsolvent induced phase separation (NIPS), which is also known as wet phase inversion, has been designed in recent years.[30−33] Unlike the conventional dip-coating, where the polymer solution on the substrates (e.g., Mg substrates) is left to evaporate directly under proper atmosphere, resulting in vitrification and formation of dense coatings, in NIPS, the polymer solution on the substrates is not left to dry but immersed in a nonsolvent of the polymer, leading to the precipitation of polymer networks. Since the mutual affinity (or miscibility) between solvent and nonsolvent (polymer should also be considered for most circumstances) will affect the demixing rate, different membrane structures could be obtained by the NIPS process. The mechanism of the NIPS process has been illustrated with a ternary phase diagram.[30,31] Generally, high mutual affinity between solvent and nonsolvent are more likely inducing instantaneous demixing, thus leading to the formation of a more porous membrane, while low mutual affinity between them would result in the reverse result.[31,34,35] For example, cellulose acetate (CA) could be dissolved in acetone, dioxane, dimethylformamide (DMF), dimethyl sulfoxide (DMSO), or tetrahydrofuran (THF) to establish a stable casting solution. Since the mutual affinity with water decreases in the order of DMSO > DMF > dioxane > acetone > THF, the tendency toward a delayed demixing process (water as nonsolvent) increases following the same sequence.[35] As a result, instantaneous demixing occurs, when DMSO, DMF, and dioxane are used as solvents, leading to the formation of a porous membrane. However, CA/acetone/water and CA/THF/water systems would provide a sponge-like membrane with a dense surface. In the study reported by Chen et al., the structures of poly(methyl methacrylate) (PMMA) membranes made from 13 different solvent/nonsolvent pairs were studied.[36] The authors reported that most of the membranes prepared by using hexane as nonsolvent featured an asymmetric structure with a dense surface and a sponge-like structure. However, when water was used as nonsolvent, PMMA dissolved in *N*-methyl-2-pyrrolidone (NMP) and dimethylacetamide would form porous structures with finger-like voids, while the PMMA that had been dissolved in acetone would form a symmetric porous structure. Biodegradable polymers demonstrate a similar phase separation process.[37−39] For instance, porous membranes with cellular morphologies could be obtained from the poly(L50/D50-lactide)/dioxane/water system.[39] However, membranes with very large macrovoids and a thin and dense

DOI: 10.1021/acs.langmuir.8b02322
Langmuir 2018, 34, 10684−10693

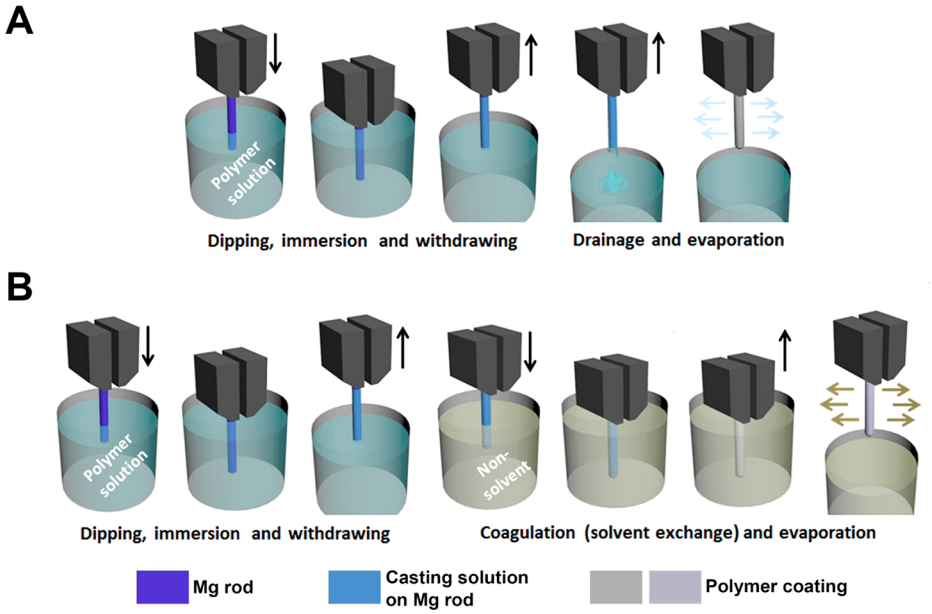

Figure 1. Illustration of (A) traditional dip-coating method combined with solvent evaporation and (B) modified dip-coating method combined with nonsolvent induced phase separation.

top layer were obtained from the poly(L50/D50-lactide)/NMP/water system. These published studies all demonstrated that the proper choice of the solvent/nonsolvent pair in accordance with polymer would greatly affect membrane morphologies.

Therefore, we herein conducted the NIPS to fabricate different PLLA coatings on pure Mg rods. We first studied the influence of different nonsolvents on the morphologies of PLLA coatings. Furthermore, the relationship between their structures and protection capability in biological fluids were investigated, and a comparison was conducted between these NIPS induced coatings and conventional evaporation induced coatings. We then investigated how coating morphologies would affect their resulting corrosion behaviors to provide insight of the corrosion mechanism of Mg implants during immersion in the physiological conditions in vitro that would simulate in vivo environment.

EXPERIMENTAL SECTION

Materials. Pure Mg rods (diameter of 1.1 mm and 99.99% purity) were obtained from the Dongguan Eontec Company, PR China. PLLA with an average molecular weight of 318 700 g/mol was provided by the Changchun SinoBiomaterials Company, PR China. Standard D-Hank's solution was obtained from the Beijing Leagene Biotechnology Company, PR China. Acetone and 1,4-dioxane were obtained from the Duksan Pure Chemical Company, South Korea. Ethanol and *n*-hexane originated from VWR Chemical. Petroleum ether (boiling point: 60 to 80 °C) was obtained from BDH Company, India.

Substrate Pretreatment. Pure Mg was chosen as substrate to validate corrosion rates and corrosion behaviors under test conditions. Mg rods were first manufactured into smaller rods with dimensions of 1.1 mm in diameter and 1.5 mm in length for our in vitro experiment. Prior to polymer disposition, all Mg rods were mechanically polished via 1000 grit waterproof abrasive paper. Thereafter, the rods were ultrasonically cleaned in acetone and pure ethanol for 20 min to remove residual contaminants. Finally, they were rinsed with pure ethanol and dried via nitrogen gas flow prior to use.

Traditional Dip-Coating Method. The 4.0 wt % PLLA solution was first prepared by dissolving PLLA in purified 1,4-dioxane and gently stirred for 12 h at room temperature. The pretreated Mg rods were then immersed into PLLA solution for 30 s to allow wetting and were subsequently slowly withdrawn from the solution to obtain a smooth wet layer of polymer solution on the Mg substrates (as shown in Figure 1A). After 1 h of hang-drying, the magnesium rods were converted, and their uncoated sides were treated in the same way, resulting in fully coated samples (for electrochemical corrosion tests, all magnesium rods were half-coated only). After full drying, magnesium rods were placed in a vacuum oven (10 mbar) for 12 h at room temperature and then underwent a thermo-process lasting 1 day at 60 °C to allow solvent evaporation.

Nonsolvent Induced Phase Separation Coatings. Pretreated Mg rods were first immersed in polymer solution for 30 s to allow wetting and then slowly withdrawn from the solution. Subsequently, the Mg rods were transported into the nonsolvent bath (coagulation bath) for the wet phase inversion process as soon as possible (as shown in Figure 1B). After 30 min of immersion and 2 h of drying, the Mg rods were converted, and the uncoated sides of the Mg rods were treated in the same way, resulting in fully coated samples. After complete drying, the coated Mg rods were placed in a vacuum oven (10 mbar) for 12 h at room temperature and then underwent a thermo-process that lasted 1 day at 60 °C to allow solvent and nonsolvent evaporation. In this part, four different organic solvents, including acetone, ethanol, hexane, and petroleum ether, were chosen as nonsolvents.

Electrochemical Corrosion Tests. Potentiodynamic polarization curves were measured via an electrochemical workstation (Versa-STAT 3, Princeton Applied Research, U.S.A.). Electrochemical corrosion tests were conducted in 50 mL of D-Hank's solution at 37 °C with an electrochemical workstation with a trielectrode cell: a magnesium rod was used as the working electrode, a platinum plate was used as the counter-electrode, and a saturated calomel electrode (SCE) was used as the reference electrode. All samples were sealed via silicon rubber sheath with an uncovered working surface area of 0.355 cm^2 (1 cm in length in the solution) and were immersed in D-Hank's solution for 15 min before the measurements started. Potentiodynamic polarization curves were scanned from −2 to −1 V at a scan rate of 5 mV/s. Both natural corrosion current (I_{corr}) and natural corrosion potential (E_{corr}) were determined with the Tafel extrapolation.[40]

In Vitro Degradation Tests. The corrosion resistance of PLLA-coated Mg rods was also evaluated via immersion tests, which were conducted in simulated body fluid (SBF) for up to 14 days. Typically, after sterilization with 75% ethanol, 6 of each of the Mg rods were

DOI: 10.1021/acs.langmuir.8b02322
Langmuir 2018, 34, 10684−10693

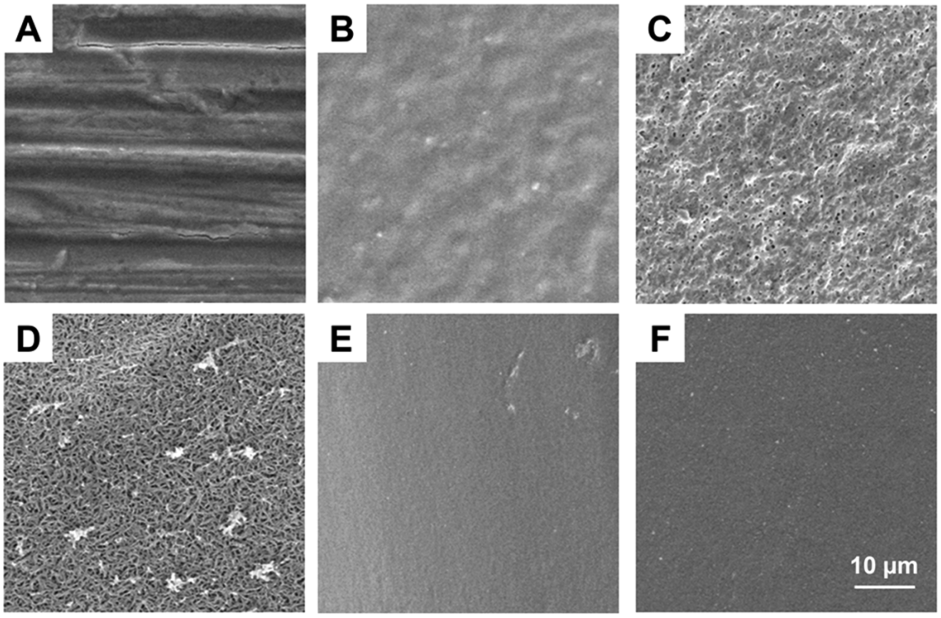

Figure 2. SEM images of surface morphologies of (A) pure magnesium (Mg); (B) solvent evaporation induced coating; NIPS induced coatings obtained via (C) acetone, (D) ethanol, (E) hexane, and (F) petroleum ether. The scale bar applies to all of the figures here.

individually introduced into parallel conical flasks with 15.0 mL of D-Hank's solution at 37 °C, respectively. The initial pH value of the solution was 7.4 and the initial concentration of the Mg ions (Mg^{2+}) was 0 ppm (ppm), with a ratio of specimen surface area (cm^2) to solution volume (mL) of around 0.036. During immersion, the soaking solution was quantitatively extracted at different time intervals, and fresh D-Hank's solution was added to maintain a constant volume. The pH value of the immersion medium was monitored with a pH meter (Orion 3-Star model, Thermo Scientific, U.S.A.), while the concentration of Mg^{2+} was monitored via an Inductively coupled plasma-optical emission spectrometer (ICP-OES, Optima 8000, PerkinElmer, U.S.A.). Samples as-soaked in the buffer for various time intervals were extracted after both 7 and 14 days of immersion, rinsed with distilled water, and dried via freeze-drying. The surface morphologies of samples (sputter coated with Au) were identified via scanning electron microscopy (SEM, Quanta-400, FEI, U.S.A.) at an accelerating voltage of 5 or 10 kV.

To obtain a direct characterization of the degradation status of Mg substrates, pure Mg rods, PLLA-coated Mg rods with traditional dip-coating, and NIPS coating were collected, and volume evaluation was conducted via Micro-CT (viva-CT40, Scanco Medical, Switzerland) scanning at time points 7, 14, and 28 days of immersion. With reconstruction, this Micro-CT scanning system was able to obtain 3D models of the skeletons.

RESULTS AND DISCUSSION

Morphology Analysis. Figure 2 shows the surface morphologies of the pure Mg substrate and the polymer-coated samples under SEM. Apparent indentations were detected on the surface of pure Mg, which was a result of substrate polishing. However, no abrasive tracks could be observed on any of the Mg substrate surfaces with polymer coatings, implying that the Mg surface had been successfully coated with PLLA via dip-coating combined with both dry and NIPS. Except for the success of polymer depositions, the SEM images also demonstrated that various morphologies could be fabricated via different nonsolvent systems. For instance, dioxane has low mutual affinity with nonpolar solvents, which caused delayed demixing. As a result, PLLA coatings with dense and nonporous surface could be achieved via using nonpolar solvents (Figure 2E,F),[36] such as hexane and ether, which resulted in very similar surfaces to those were induced via solvent evaporation (Figure 2B). However, using polar solvents, such as ethanol and acetone, PLLA coatings with porous surface could be achieved (Figure 2C,D),[41] due to instantaneous demixing. Furthermore, it was also demonstrated that the pore size could easily be varied via different nonsolvents. For example, acetone contributed to the formation of individual small pores, while ethanol would result in the formation of interconnected pores. In addition to surface morphology, NIPS also had a great influence on the inner structures of coating, where large amounts of voids could be found within the membranes. This is very different from the three-layer structure of the dry phase inversion induced by polymer coatings.[25] Furthermore, ether induced coating has thinner outer layers than hexane induced coating, which might be the result of different solvent/nonsolvent diffusion rates. Thus, through the NIPS process, we controlled both morphology and structure of coatings by simply changing the solvent/nonsolvent system, which provided an effective and efficient way to control the degradation of the magnesium implants. More importantly, due to the simple removal of the solvent via solvent/nonsolvent exchange, solvents with high boiling points could be introduced into the coating system, thus greatly expanding the varieties of applicable polymers.[35,36]

Electrochemical Measurement. To investigate the corrosion resistance of all samples, electrochemical corrosion tests were conducted for the uncoated and coated substrates,[12] as shown in Figure 3 and Table 1. It was apparent that all polymer coatings on the Mg rods resulted in lower I_{corr} values and/or more anodic E_{corr} values when compared to pure Mg rods, illustrating that all coatings could improve the corrosion resistance of the Mg substrate. However, the results implied that nonpolar solvent induced PLLA coatings would offer the greatest reduction in corrosion current over uncoated coatings; their corrosion currents were too low for measuring. Dry phase inversion induced coatings (red curve) with dense structures also demonstrated a comparatively positive corrosion potential; however, their corrosion current was high, indicating that

DOI: 10.1021/acs.langmuir.8b02322
Langmuir 2018, 34, 10684−10693

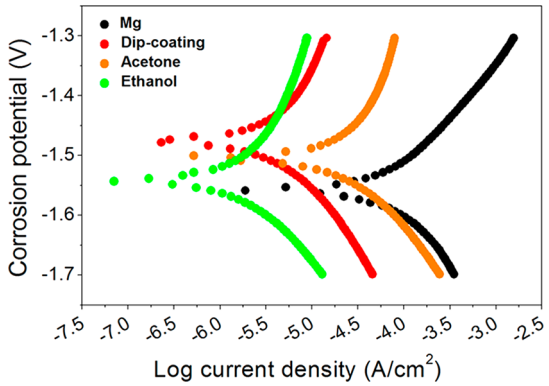

Figure 3. Potentiodynamic polarization curves of all PLLA-coated and uncoated magnesium rods, which were obtained from the electrochemical measurement after they were immersed in D-Hank's solution.

Table 1. Corrosion Potential (E_{corr}) and Current Density (I_{corr}) Values for Coated and Uncoated Substrates

	Mg	dip-coating	acetone	ethanol	hexane	petroleum ether
E_{corr} (V)	−1.55	−1.46	−1.52	−1.53	very low current density was detected, indicating extremely slow corrosion rate	
I_{corr} (μA/cm^2)	87.1	8.55	39.3	1.88		

microdefects existed in these PLLA coatings. Compared to coatings with dense surface, porous coatings (green curve and orange curve) demonstrated negative E_{corr}, although they still retained a comparatively low I_{corr}. Since E_{corr} was associated with the activity of the Mg substrate, one possible reason is that these porous membranes could not prevent water molecules from passing through and further reacting with the substrates. However, since PLLA coatings could contribute to the formation of polymer/mineral layers, which provide a secondary protection to the substrates, all these coatings still have very low I_{corr}, implying their ability to greatly slow the corrosion rates of the substrates. Thus, the protective properties of the coatings can be adjusted by controlling their morphologies as well as structures via different phase inversion processes.

In Vitro Immersion Tests. To better investigate the corrosion rates of Mg rods, the pH change and Mg^{2+} released from the samples were investigated,[12] as shown in Figures 4−6. During the whole immersion time, up to 26 ppm of Mg^{2+} were released from the uncoated samples over 14 days (Figure 4), which was more than 6 times that of the coated samples (Figure 5). Furthermore, the slowing of the constant fast release of Mg^{2+} from uncoated samples implied the formation of mineral layers.[42] However, these layers could not provide good protection for the substrates, since these loosely packed sediments would be quickly destroyed by chloride ions and formed hydrogen bubbles.[11,43] The results of pH changes followed the same trend as those of the release of Mg^{2+}. It could be detected that substantially low pH values were retained on the polymer coated samples compared to the uncoated samples during the whole immersion period, and the disparities became much larger at a later stage.

Although all PLLA coatings provided good protection for the substrates, the results demonstrated that different polymer

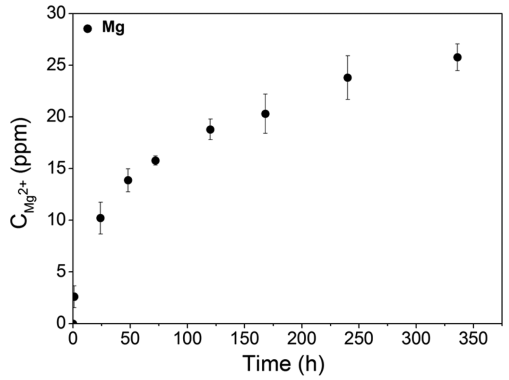

Figure 4. Release of Mg^{2+} from uncoated pure Mg rods over time after immersion in D-Hank's solution (n = 3).

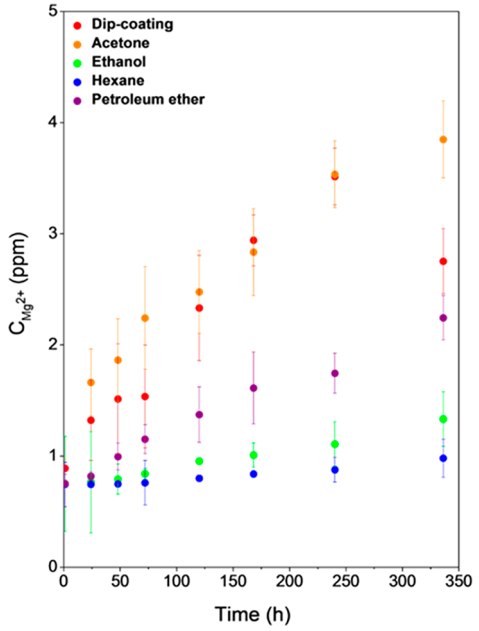

Figure 5. Release of Mg^{2+} from PLLA-coated pure Mg rods over time after immersion in D-Hank's solution (n = 3).

coatings would contribute to varied corrosion improvement at different levels. As shown in Figure 5, hexane induced PLLA coatings offered the best protection for Mg substrates, which released only 0.98 ppm Mg^{2+} after a 14-day immersion, followed by ethanol induced PLLA coatings, which had a similar release at a value of 1.33 ppm. In contrast, dry phase inversion induced samples and acetone induced samples showed a higher amount of Mg^{2+} release into the media after a 14-day immersion, with larger pH changes at the same time. However, due to the low ratios of specimen surface area (cm^2) to solution volume (mL), in combination with the buffer effect of the D-Hank's solution, their variation is not remarkable. In addition to faster corrosion rates, solvent evaporation induced samples and acetone induced samples all showed a sudden increase of Mg^{2+} release during immersion, which were very different to other samples.

In Vitro CT Tests. The in vitro corrosion of the implants was investigated via micro-CT tomography. Figures 7 and 8 show the 3D models of the Mg rods after the reconstructions, in combination with the changes of their volumes and density. For the CT images, it could be shown that pure Mg rods

DOI: 10.1021/acs.langmuir.8b02322
Langmuir 2018, 34, 10684−10693

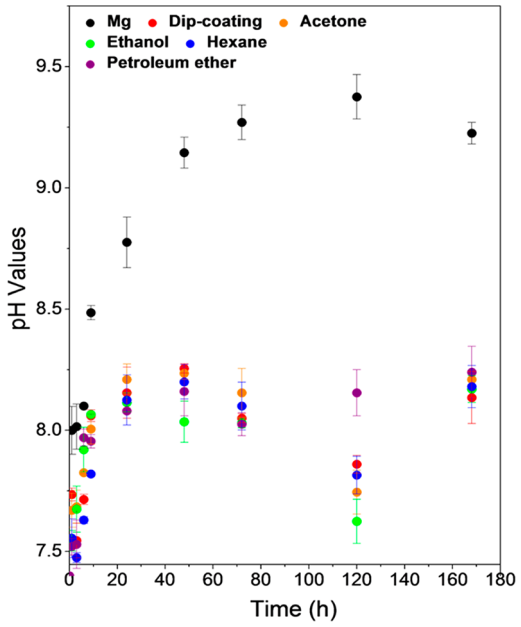

Figure 6. pH values of PLLA-coated and uncoated pure Mg rods over time after immersion in D-Hank's solution (n = 3).

experienced fast corrosion after immersion, while the polymer coatings could enhance the corrosion resistance of the substrates even after a 4-week immersion, which was very similar to the trend of in vitro Mg^{2+} release. Further, as shown in Figure 8, pure Mg rods underwent relatively fast increase in density and loss of volume in the first 2 weeks, indicating the rapid corrosion of uncoated Mg substrates. Due to dissolution of the Mg rods, the total volume of the Mg rods decreased with the immersion time. Simultaneously, fast precipitation of magnesium apatite around the Mg substrates was induced by the explosive release of Mg^{2+}, leading to the fast increase in their density. Since the apparent volume of Mg rods would be padded by the formed mineral layer, the actual corrosion rates might be even faster. For long-term immersion, since the mineral layer would slowly peel off from the substrate, the apparent volume of the Mg rods expanded, while their density started to decrease finally. In contrast, coated Mg rod showed only obscure changes in the first week, indicating the excellent isolation provided by all PLLA coatings. However, after 2 weeks, the dense PLLA coatings were found to lose their protection capacity, resulting in the dissolution of the Mg substrates and precipitation of magnesium apatite around the substrate. More seriously, a rapid decrease in both volume and density was also observed in the coated Mg rod induced by solvent evaporation, indicating the dense PLLA coatings were unfavorable to provide long-term protection to the substrates. In comparison, the density of coated Mg rod induced via hexane induced nonsolvent phase inversion slightly decreased with the immersion time, indicating slow corrosion rates and Mg^{2+} release. Since the concentration of Mg^{2+} was extremely low around the Mg rods, mineral could be formed apart from the substrates, resulting in a expansion of the apparent volume. More importantly, the results indicated that a stable mineral/polymer composite structure would be formed during the long-term immersion, which could provide further protection to the substrates. As a result, the change of volume and density of coated Mg rod induced by nonsolvent phase inversion became more ignorable after long-term immersion test.

Mechanism of Mg Corrosion. To better illustrate the differences between these phenomena, we investigated morphological changes of the samples during immersion at different time intervals. Figure 9 shows the surface morphologies of the coatings after soaking in D-Hank's solution for 7 days. Figure 9A shows the appearance of apparent mineral layers on the surface of magnesium rods after 7-day immersion,[42] which would enhance the corrosion resistance of substrates, resulting in slower corrosion rates after long-time immersion. However, their multilayer structure

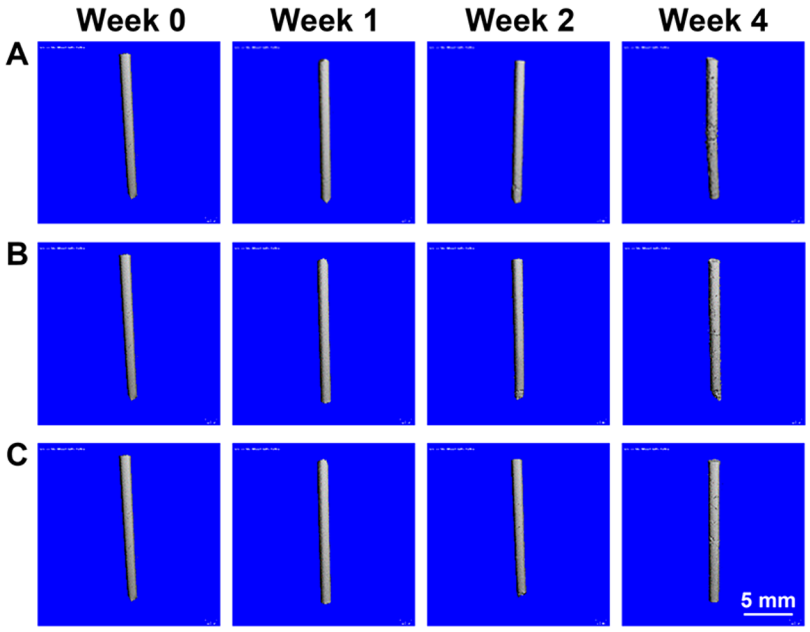

Figure 7. Micro-CT reconstruction images of (A) the uncoated pure magnesium (Mg) rod, (B) the coated Mg rod induced by solvent evaporation, and (C) the coated Mg rod induced via hexane induced wet phase inversion over time after immersed in D-Hank's solution. The scale bar applies to all of the figures here.

DOI: 10.1021/acs.langmuir.8b02322
Langmuir 2018, 34, 10684−10693

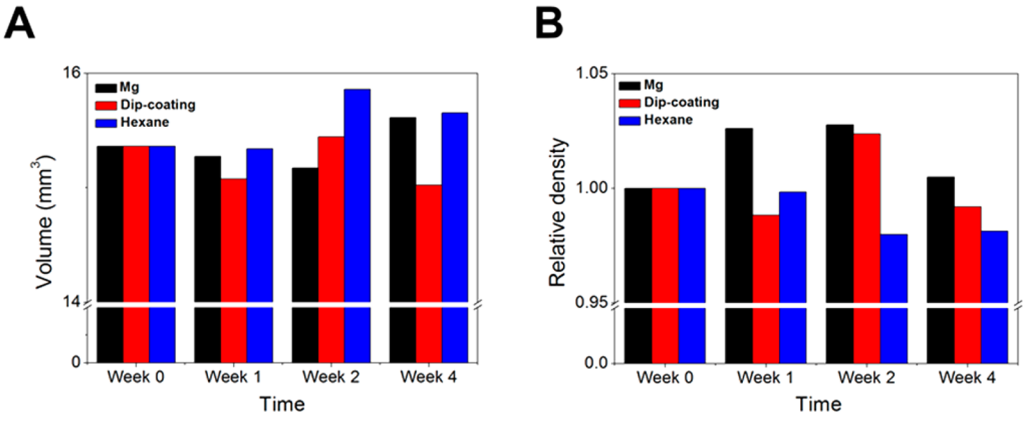

Figure 8. Change of (A) volume and (B) relative density of PLLA-coated and uncoated pure magnesium (Mg) rods over time calculated via micro-CT.

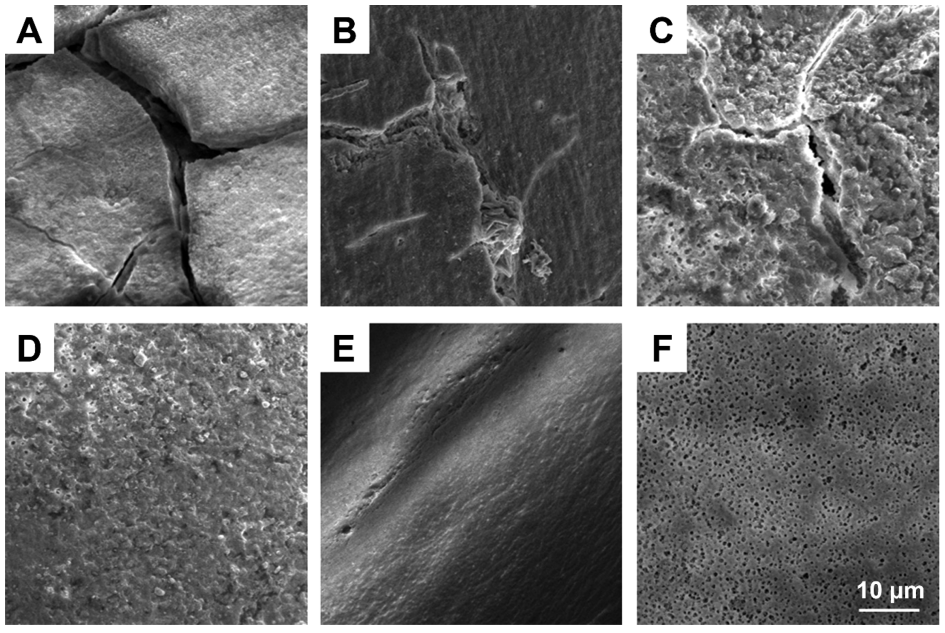

Figure 9. SEM images of surface morphologies of (A) pure magnesium (Mg); (B) solvent evaporation induced coating; NIPS induced coatings via (C) acetone, (D) ethanol, (E) hexane, and (F) petroleum ether after 7-day immersion. The scale bar applies to all of the figures here.

implies that these loose-packed sediments could not provide sufficient protection to the substrates due to large defects and poor adhesion. Compared to uncoated samples, PLLA-coated rods demonstrated a more complex corrosion behavior. For polymer coatings with dense surface and porous inner structures, only small defects could be found (Figure 9E,F), as a result of hydrolysis and dissolution of the PLLA polymer during immersion tests. However, for coatings without inner pores, such as dry phase inversion induced coatings (Figure 9B) and acetone induced coatings (Figure 9C), huge cracks formed due to the blast of hydrogen bubbles, consequently resulting in the loss of their capability to protect substrates, along with a sudden release of Mg^{2+} and change of pH.[25] This could also be further underpinned by the completeness of porous coating induction by ethanol. Although water molecules would rapidly pass through the ethanol induced coatings, their porous structures, which could excrete the formed hydrogen bubbles at an identical same rate, could still maintain their integrity.[25,29] More importantly, SEM images clearly shows that a large amount of minerals formed under/inside the membranes, since PLLA helped to mineralize magnesium ions.[44]

With the help of the polymer network, which would contribute to the formation of polymer/mineral composites, corrosion products would have positive effects on their long-term capability,[25,27,29,45] as shown in Figure 10. After a 14-day immersion, solvent evaporation induced coatings, along with acetone induced coatings, broke into pieces, which resulted in relatively high corrosion rates after long time immersion. However, due to the formation of polymer/mineral composites, which could prevent the minerals from falling off, both groups still demonstrated improved corrosion resistance compared to uncoated samples. In contrast, no peeling off of other coating films was observed during soaking in the D-Hank's solution even after a 14-day immersion, although defects and minerals were detected on these coatings. The integrity of the protective layers led to far lower corrosion rates. This detailed mechanism, which includes substrate corrosion, hydrolysis of polymers, and formation of polymer/mineral composites, strongly confirms that the polymer

DOI: 10.1021/acs.langmuir.8b02322
Langmuir 2018, 34, 10684−10693

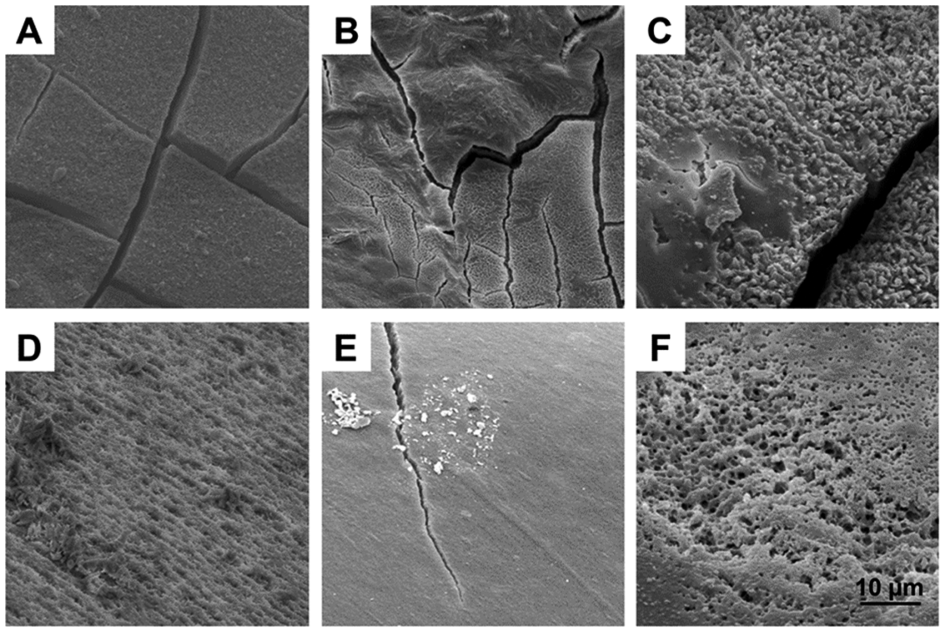

Figure 10. SEM images of surface morphologies of (A) pure magnesium (Mg); (B) solvent evaporation induced coating; NIPS induced coatings via (C) acetone, (D) ethanol, (E) hexane, and (F) petroleum ether after 14-day immersion. The scale bar applies to all of the figures here.

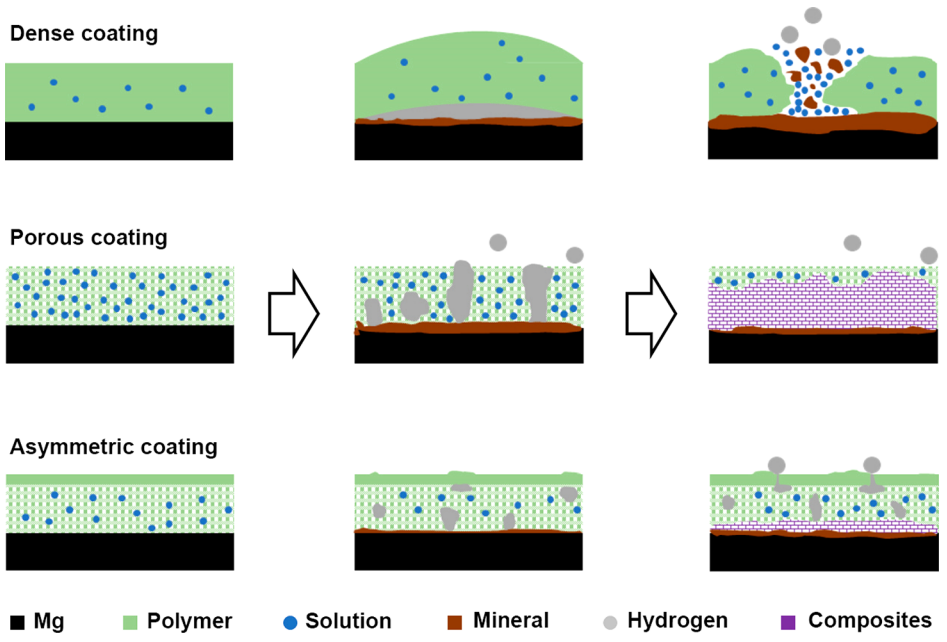

Figure 11. Illustration of the mechanism of Mg corrosion with different PLLA coatings.

coatings not only play an important role for initial protection but have also participated in the formation of polymer/mineral composites, which can enhance the long-term corrosion resistance. Thus, all PLLA coated samples showed very low corrosion rates, even after extended immersion.

As illustrated in Figure 11 and Table 2, PLLA coatings with dense surface strongly prevented water molecules from passing through, resulting in low initial corrosion rates and higher anodic E_{corr} values. However, magnesium substrates would slowly corrode in the buffer solution, although coating enhanced their corrosion resistance. Therefore, at this stage, the three-dimensional (3D) structures of coatings posed a more important influence on their protection capabilities, reflecting that coatings with inner pores provided better protection due to their ability to maintain their integrity. This is why dry phase inversion induced coatings as well as acetone induced coatings demonstrated comparatively high corrosion

Table 2. Illustration of Effects of Polymer Coatings on Their Protection Capabilities

nonsolvent	surface	3D structure	first stage	second stage	third stage
air (dry phase inversion)	dense	low porosity	+	−	+
acetone	porous	low porosity	−	−	−
ethanol	porous	high porosity	−	+	+
hexane	dense	high porosity	+	+	+
petroleum ether	dense	high porosity	+	+	+

DOI: 10.1021/acs.langmuir.8b02322
Langmuir 2018, 34, 10684−10693

rates after short-time immersion. During the last stage (typically for long-term immersion), the composite layers would provide further protection to the substrates. Since all polymer coatings contributed to the formation of polymer/mineral composites, all polymer coatings could provide long-term protection to substrates as opposed to the pure magnesium rods; this could also be reflected in lower I_{corr} values of all PLLA-coated samples. This novel mechanism perfectly explains why different coatings all provide some corrosion protection to the substrates, without passivating the substrate from corrosion at the same extent. This would further benefit the design and improvement of already very good coatings for Mg implants.

CONCLUSION

To conclude, we developed a novel method, which combines the NIPS process with the traditional dip-coating method, to fabricate biodegradable PLLA coatings on magnesium (Mg) substrates. Unlike conventional dip-coating, where the phase separation is induced via solvent evaporation, the phase separation of a polymer solution in wet casting is induced via immersion of the polymer solution in a coagulation bath of the nonsolvent. The current study demonstrated that a careful selection of nonsolvents could effectively control the polymer coating morphologies and inner structures, resulting in a wide variety of protective layers on the surface of Mg alloys. PLLA coatings with a dense surface were obtained from dioxane/hexane and dioxane/petroleum ether systems, while PLLA coatings with a porous surface were obtained from dioxane/acetone and dioxane/ethanol systems. In contrast, PLLA coatings with a symmetric and dense structure were obtained from EIPS. All PLLA coatings prepared on the Mg rods successfully improved the corrosion resistance of substrates, while PLLA films obtained via wet casting had lower pH changes and slower Mg^{2+} release and showed a more stable trend than uncoated samples and samples coated via a standard dry casting technique, implying better protective effects of coatings that have been achieved via the wet phase inversion method. The latter prevented penetration of body fluid, since they affected the formation of the polymer/mineral composite. This indicates that coatings with dense surface and high inner porosity would be an ideal candidate for long-term protection. Since the structures of the polymer coatings could be regulated to control the corrosion rate of Mg substrates, this method would greatly broaden the application of polymer coating on Mg-based implants for various biomedical requirements.

AUTHOR INFORMATION

Corresponding Authors

*E-mail: tongai@cuhk.edu.hk.

*E-mail: qin@ort.cuhk.edu.hk.

ORCID

Chi Wu: 0000-0002-5606-4789

To Ngai: 0000-0002-7207-6878

Notes

The authors declare no competing financial interest.

ACKNOWLEDGMENTS

The financial support of this work by the Hong Kong Special Administration Region (HKSAR) Collaborative Research Fund (CRF 2014/15-C4028-14GF) and General Research Fund (CUHK14303715, 2130429) is gratefully acknowledged.

REFERENCES

(1) LeGeros, R. Z. Materials for Bone Repair, Augmentation, and Implant Coatings. In *Biomechanics in Orthopedics*; Niwa, S., Perren, S. M., Hattori, T., Eds.; Springer Japan: Tokyo, 1992; pp 147−174.

(2) Saini, M.; Singh, Y.; Arora, P.; Arora, V.; Jain, K. Implant biomaterials: A comprehensive review. *World J. Clin. Cases* **2015**, *3* (1), 52−57.

(3) Navarro, M.; Michiardi, A.; Castaño, O.; Planell, J. A. Biomaterials in orthopaedics. *J. R. Soc., Interface* **2008**, *5* (27), 1137−1158.

(4) Staiger, M. P.; Pietak, A. M.; Huadmai, J.; Dias, G. Magnesium and its alloys as orthopedic biomaterials: A review. *Biomaterials* **2006**, *27* (9), 1728−1734.

(5) Gu, X.; Zheng, Y. A review on magnesium alloys as biodegradable materials. *Front. Mater. Sci. China* **2010**, *4* (2), 111−115.

(6) Poinern, G. E. J.; Brundavanam, S.; Fawcett, D. Biomedical magnesium alloys: a review of material properties, surface modifications and potential as a biodegradable orthopaedic implant. *Am. J. Biomed. Eng.* **2012**, *2* (6), 218−240.

(7) Ridzwan, M.; Shuib, S.; Hassan, A.; Shokri, A.; Ibrahim, M. M. Problem of stress shielding and improvement to the hip implant designs: a review. *J. Med. Sci.* **2007**, *7* (3), 460−467.

(8) Barber, F. A.; Dockery, W. D. Long-Term Absorption of Poly-L-Lactic Acid Interference Screws. *Arthroscopy* **2006**, *22* (8), 820−826.

(9) Zhao, D.; Witte, F.; Lu, F.; Wang, J.; Li, J.; Qin, L. Current status on clinical applications of magnesium-based orthopaedic implants: A review from clinical translational perspective. *Biomaterials* **2017**, *112*, 287−302.

(10) Witte, F.; Kaese, V.; Haferkamp, H.; Switzer, E.; Meyer-Lindenberg, A.; Wirth, C. J.; Windhagen, H. In vivo corrosion of four magnesium alloys and the associated bone response. *Biomaterials* **2005**, *26* (17), 3557−3563.

(11) Zeng, R.; Dietzel, W.; Witte, F.; Hort, N.; Blawert, C. Progress and Challenge for Magnesium Alloys as Biomaterials. *Adv. Eng. Mater.* **2008**, *10* (8), B3−B14.

(12) Kirkland, N. T.; Birbilis, N.; Staiger, M. P. Assessing the corrosion of biodegradable magnesium implants: A critical review of current methodologies and their limitations. *Acta Biomater.* **2012**, *8* (3), 925−936.

(13) Zhao, D.; Huang, S.; Lu, F.; Wang, B.; Yang, L.; Qin, L.; Yang, K.; Li, Y.; Li, W.; Wang, W.; Tian, S.; Zhang, X.; Gao, W.; Wang, Z.; Zhang, Y.; Xie, X.; Wang, J.; Li, J. Vascularized bone grafting fixed by biodegradable magnesium screw for treating osteonecrosis of the femoral head. *Biomaterials* **2016**, *81*, 84−92.

(14) Zhang, Y.; Xu, J.; Ruan, Y. C.; Yu, M. K.; O'Laughlin, M.; Wise, H.; Chen, D.; Tian, L.; Shi, D.; Wang, J.; Chen, S.; Feng, J. Q.; Chow, D. H. K.; Xie, X.; Zheng, L.; Huang, L.; Huang, S.; Leung, K.; Lu, N.; Zhao, L.; Li, H.; Zhao, D.; Guo, X.; Chan, K.; Witte, F.; Chan, H. C.; Zheng, Y.; Qin, L. Implant-derived magnesium induces local neuronal production of CGRP to improve bone-fracture healing in rats. *Nat. Med.* **2016**, *22*, 1160.

(15) Krause, A.; von der Höh, N.; Bormann, D.; Krause, C.; Bach, F. W.; Windhagen, H.; Meyer-Lindenberg, A. Degradation behaviour and mechanical properties of magnesium implants in rabbit tibiae. *J. Mater. Sci.* **2010**, *45* (3), 624−632.

(16) Hornberger, H.; Virtanen, S.; Boccaccini, A. R. Biomedical coatings on magnesium alloys − A review. *Acta Biomater.* **2012**, *8* (7), 2442−2455.

(17) Wang, J.; Tang, J.; Zhang, P.; Li, Y.; Wang, J.; Lai, Y.; Qin, L. Surface modification of magnesium alloys developed for bioabsorbable orthopedic implants: A general review. *J. Biomed. Mater. Res., Part B* **2012**, *100B* (6), 1691−1701.

(18) Wu, G.; Ibrahim, J. M.; Chu, P. K. Surface design of biodegradable magnesium alloys — A review. *Surf. Coat. Technol.* **2013**, *233*, 2−12.

(19) Gray, J. E.; Luan, B. Protective coatings on magnesium and its alloys — a critical review. *J. Alloys Compd.* **2002**, *336* (1−2), 88−113.

DOI: 10.1021/acs.langmuir.8b02322
Langmuir 2018, 34, 10684−10693

(20) Li, N.; Zheng, Y. Novel Magnesium Alloys Developed for Biomedical Application: A Review. *J. Mater. Sci. Technol.* **2013**, *29* (6), 489−502.
(21) Tang, J.; Wang, J.; Xie, X.; Zhang, P.; Lai, Y.; Li, Y.; Qin, L. Surface coating reduces degradation rate of magnesium alloy developed for orthopaedic applications. *J. Orthop. Transl.* **2013**, *1* (1), 41−48.
(22) Wong, H. M.; Yeung, K. W. K.; Lam, K. O.; Tam, V.; Chu, P. K.; Luk, K. D. K.; Cheung, K. M. C. A biodegradable polymer-based coating to control the performance of magnesium alloy orthopaedic implants. *Biomaterials* **2010**, *31* (8), 2084−2096.
(23) Li, J.; Cao, P.; Zhang, X.; Zhang, S.; He, Y. In vitro degradation and cell attachment of a PLGA coated biodegradable Mg−6Zn based alloy. *J. Mater. Sci.* **2010**, *45* (22), 6038−6045.
(24) Xu, L.; Yamamoto, A. Characteristics and cytocompatibility of biodegradable polymer film on magnesium by spin coating. *Colloids Surf., B* **2012**, *93*, 67−74.
(25) Abdal-hay, A.; Barakat, N. A. M.; Lim, J. K. Influence of electrospinning and dip-coating techniques on the degradation and cytocompatibility of Mg-based alloy. *Colloids Surf., A* **2013**, *420*, 37−45.
(26) Scharnagl, N.; Blawert, C.; Dietzel, W. Corrosion protection of magnesium alloy AZ31 by coating with poly(ether imides) (PEI). *Surf. Coat. Technol.* **2009**, *203* (10−11), 1423−1428.
(27) Conceicao, T. F.; Scharnagl, N.; Blawert, C.; Dietzel, W.; Kainer, K. U. Corrosion protection of magnesium alloy AZ31 sheets by spin coating process with poly(ether imide) (PEI). *Corros. Sci.* **2010**, *52* (6), 2066−2079.
(28) Gu, X.; Zheng, Y.; Lan, Q.; Cheng, Y.; Zhang, Z.; Xi, T.; Zhang, D. Surface modification of an Mg-1Ca alloy to slow down its biocorrosion by chitosan. *Biomed. Mater.* **2009**, *4* (4), 044109.
(29) Kim, S. B.; Jo, J. H.; Lee, S. M.; Kim, H. E.; Shin, K. H.; Koh, Y. H. Use of a poly(ether imide) coating to improve corrosion resistance and biocompatibility of magnesium (Mg) implant for orthopedic applications. *J. Biomed. Mater. Res., Part A* **2013**, *101A* (6), 1708−1715.
(30) Ismail, A. F.; Yean, L. P. Review on the development of defect-free and ultrathin-skinned asymmetric membranes for gas separation through manipulation of phase inversion and rheological factors. *J. Appl. Polym. Sci.* **2003**, *88* (2), 442−451.
(31) Guillen, G. R.; Pan, Y.; Li, M.; Hoek, E. M. V. Preparation and Characterization of Membranes Formed by Nonsolvent Induced Phase Separation: A Review. *Ind. Eng. Chem. Res.* **2011**, *50* (7), 3798−3817.
(32) Lalia, B. S.; Kochkodan, V.; Hashaikeh, R.; Hilal, N. A review on membrane fabrication: Structure, properties and performance relationship. *Desalination* **2013**, *326*, 77−95.
(33) Wang, D.; Lai, J. Recent advances in preparation and morphology control of polymeric membranes formed by nonsolvent induced phase separation. *Curr. Opin. Chem. Eng.* **2013**, *2* (2), 229−237.
(34) Simone, S. Coagulation Bath. In *Encyclopedia of Membranes*; Drioli, E., Giorno, L., Eds.; Springer: Berlin, 2015; pp 1−2.
(35) Mulder, J. *Basic Principles of Membrane Technology*; Springer Netherlands: Amsterdam, 1991.
(36) Cheng, J.; Wang, D.; Lin, F.; Lai, J. Formation and gas flux of asymmetric PMMA membranes. *J. Membr. Sci.* **1996**, *109* (1), 93−107.
(37) Kim, S. Y.; Kanamori, T.; Noumi, Y.; Wang, P.; Shinbo, T. Preparation of porous poly(D,L-lactide) and poly(D,L-lactide-co-glycolide) membranes by a phase inversion process and investigation of their morphological changes as cell culture scaffolds. *J. Appl. Polym. Sci.* **2004**, *92* (4), 2082−2092.
(38) Ellis, M. J.; Chaudhuri, J. B. Poly(lactic-co-glycolic acid) hollow fibre membranes for use as a tissue engineering scaffold. *Biotechnol. Bioeng.* **2007**, *96* (1), 177−187.
(39) vandeWitte, P.; Esselbrugge, H.; Dijkstra, P. J.; vandenBerg, J. W. A.; Feijen, J. A morphological study of membranes obtained from the systems polylactide-dioxane-methanol, polylactide-dioxane-water, and polylactide-N-methyl pyrrolidone-water. *J. Polym. Sci., Part B: Polym. Phys.* **1996**, *34* (15), 2569−2578.
(40) Shi, Z.; Liu, M.; Atrens, A. Measurement of the corrosion rate of magnesium alloys using Tafel extrapolation. *Corros. Sci.* **2010**, *52* (2), 579−588.
(41) Shi, J.; Alves, N. M.; Mano, J. F. Towards bioinspired superhydrophobic poly(L-lactic acid) surfaces using phase inversion-based methods. *Bioinspiration Biomimetics* **2008**, *3* (3), 034003.
(42) Song, G. Recent Progress in Corrosion and Protection of Magnesium Alloys. *Adv. Eng. Mater.* **2005**, *7* (7), 563−586.
(43) Williams, D. New interests in magnesium. *Med. Device Technol.* **2006**, *17* (3), 9−10.
(44) Zhang, R.; Ma, P. Biomimetic Polymer/Apatite Composite Scaffolds for Mineralized Tissue Engineering. *Macromol. Biosci.* **2004**, *4* (2), 100−111.
(45) da Conceicao, T. F.; Scharnagl, N.; Dietzel, W.; Kainer, K. U. On the degradation mechanism of corrosion protective poly(ether imide) coatings on magnesium AZ31 alloy. *Corros. Sci.* **2010**, *52* (10), 3155−3157.

DOI: 10.1021/acs.langmuir.8b02322
Langmuir 2018, 34, 10684−10693